Nuclear Structure Studies in the Lead Region with Stripping Reactions*

PARESH MUKHERJEE† AND BERNARD L. COHEN
University of Pittsburgh, Pittsburgh, Pennsylvania
(Received April 9, 1962)

The seven single-particle neutron states in the $126<N\leqslant 184$ shell are located and identified with the $Pb^{208}(d,p)Pb^{209}$ reaction. The missing $h_{9/2}$ hole state in Pb^{207} is also located and identified with (d,t) reactions. Nuclei with two particles and holes, such as Pb^{206}, Pb^{208} (excited), Bi^{208}, and Bi^{210} are studied; their level structure can be qualitatively and sometimes even semi-quantitatively understood by considering two-particle couplings using the known particle and hole states. The ground-state wave function of Pb^{206} is studied by three independent methods; all agree that it is only about 54% $(p_{1/2})^{-2}$ rather than 73% as given by shell-model calculations. The three-neutron spectra of Pb^{205} and Pb^{207} (excited) are studied, and the principal features can be understood as couplings of one particle or hole to the ground state and other low-lying states of Pb^{206}. Some preliminary evidence is obtained on the $N>184$ shell.

INTRODUCTION AND EXPERIMENTAL

THE region around Pb^{208} is a most interesting one for nuclear structure studies. That nucleus is the only one in the heavy element region in which both the neutron and proton shells are closed. In addition the ratio of the energy gap between major shells to the energy gaps between the subshells seems to be larger here than in the lighter doubly closed shell nuclei (Ca^{40},O^{16}), and the j-j coupling approximation is expected to be extremely good. In view of this very clean double-closed shell behavior, the structure of nuclei with one, two, or even three particles and holes outside of Pb^{208} can be studied theoretically using shell-model techniques without questionable approximations. It is the purpose of this paper to study these nuclei with the (d,p) and (d,t) stripping reactions.

Before serious progress can be made in the theoretical work, it is essential that the single-particle and single-hole states be clearly identified. This can be done for the neutron particle and hole states by the (d,p) and (d,t) reactions, respectively, on Pb^{208}. This represents perhaps the most important part of this paper. All of the seven single-particle states in the $126<N\leqslant 184$ shell are located and identified, and the long missing $h_{9/2}$ single-hole state in the $82<N\leqslant 126$ shell is found.

The next problem is to study the structure of nuclei with two particles and holes. This is done for Pb^{206} [by $Pb^{207}(d,t)$ and $Pb^{206}(d,p)$], for Pb^{208} [by $Pb^{207}(d,p)$], for Bi^{210} [by $Bi^{209}(d,p)$], and for Bi^{208} [by $Bi^{209}(d,t)$]. In all cases, the structure can be understood qualitatively—and in some cases semi-quantitatively—by simple couplings. The ground-state wave function of Pb^{206} is studied by three different techniques; all give consistent results, but results differing markedly from published shell-model calculations. Some work is also reported on the three-neutron nuclei, Pb^{205} and Pb^{207} (highly excited states).

In two previous papers,[1] measurements of energy distributions and angular distributions of protons and tritons from (d,p) and (d,t) reactions in Pb^{206}, Pb^{207}, Pb^{208}, and Bi^{209} were used to study nuclear structure problems. While there were many interesting successes in that work, many unsolved problems remained.

Several improvements over the techniques used in reference 1 have recently become possible. Firstly, a method of preparing separated isotope targets by evaporation without undue material losses was developed,[2] so that Pb isotope targets in the thickness range 1.0–1.5 mg/cm² became available. This allowed an improvement in resolution from about 120 keV in reference 1 to about 40 keV in this work. Secondly, distorted-wave Born approximation (DWB) calculations became available[3]; these aid greatly in the analysis of (d,p) reactions. In addition, more highly enriched isotopic material was obtained, and new theoretical shell-model calculations have become available.

The experimental method was the same as that used in reference 1 except that the resolution was improved by the use of thinner targets and other techniques discussed in reference 4. An improved energy calibration[4] of the spectrograph system has also been incorporated. The targets are on a thin (0.2 mg/cm²) gold backing so that contributions from the Au must be subtracted; this process gave little difficulty. The difficulties from carbon and oxygen contamination were relatively much greater than in the previous work, but still not excessively serious. In all cases, measurements were made at several angles so that peaks due to light element impurities could easily be detected by their change in energy with angles. Typical data for (d,p) and (d,t) reactions are shown in Figs. 1 and 2.

* Supported by the National Science Foundation and the Office of Naval Research.

† On leave from Saha Institute of Nuclear Physics, Calcutta, India.

[1] B. L. Cohen, S. Mayo, and R. E. Price, Nuclear Phys. **20**, 360 (1960); B. L. Cohen, R. E. Price, and S. Mayo, *ibid.* **20**, 370 (1960).

[2] The targets were prepared by G. Fodor of this laboratory.

[3] The distorted-wave Born approximation (DWB) calculations were carried out by G. R. Satchler, R. H. Bassel, and R. M. Drisko, using the Oak Ridge Computer.

[4] B. L. Cohen, R. H. Fulmer, and A. L. McCarthy, Phys. Rev. **126**, 698 (1962).

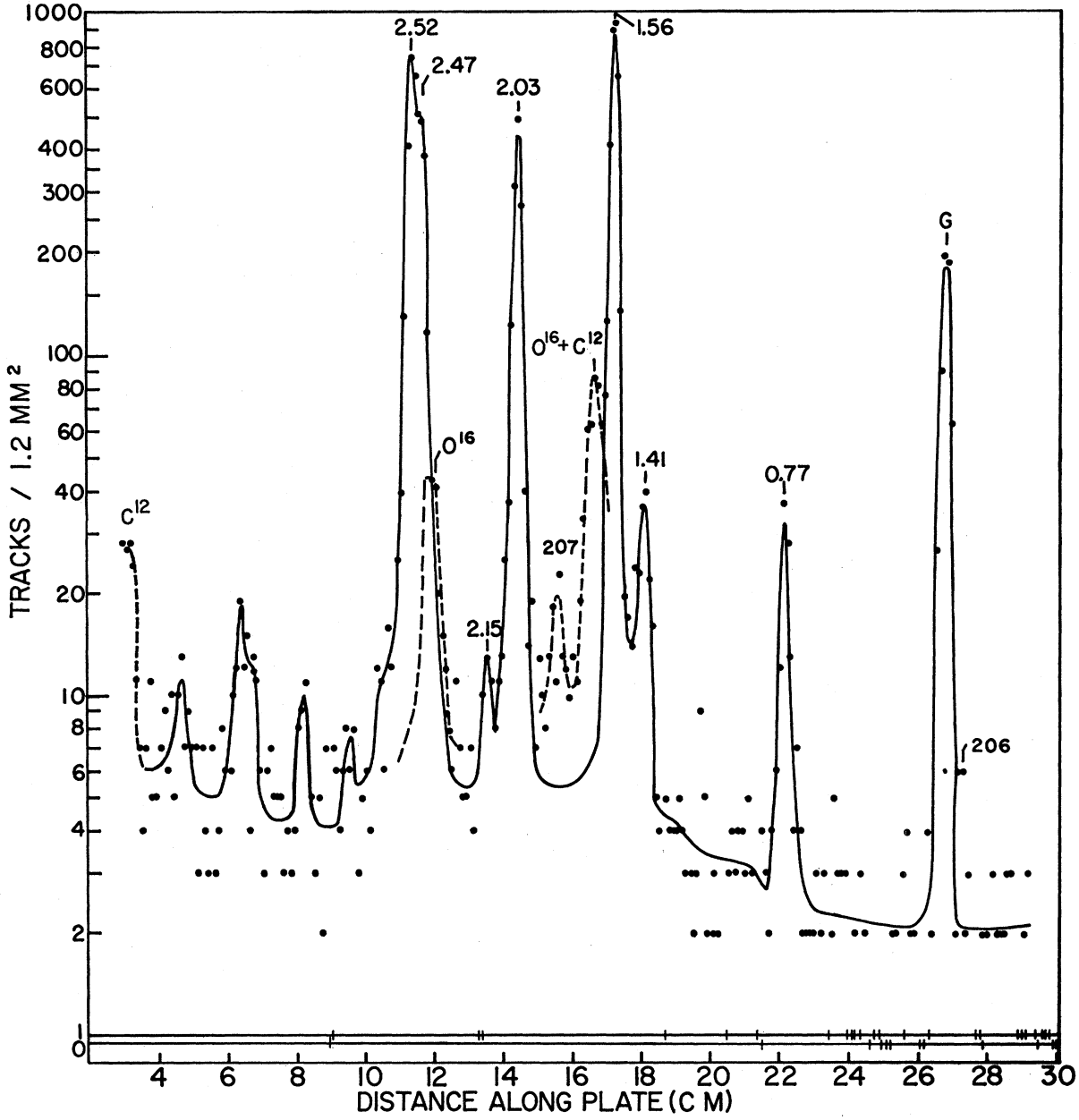

FIG. 1. Energy distribution of protons from $Pb^{208}(d,p)Pb^{209}$. Angle of observation is 75°. The numbers above the prominent proton groups are excitation energies in Pb^{209} in MeV. The spectra due to oxygen, carbon, and Pb^{207} impurities are shown by the dashed curve.

RESULTS AND DISCUSSION: (d,p) REACTIONS

A. Single-Particle Levels in $126 < N \leqslant 184$ Shell; the Pb^{209} Level Structure

The straightforward method of identifying the single-particle levels in the $126 < N \leqslant 184$ shell is from a study of the $Pb^{208}(d,p)Pb^{209}$ reaction. This was done in reference 1, but consistent results were not obtained. The principal new experimental developments here, as can be seen from Fig. 1, are the clear resolution of an additional level at 1.41-MeV excitation energy, and the recognition that the 2.5-MeV level is actually a 2.47–2.52 MeV doublet. But the most important help is the availability of DWB calculations.

The single-particle levels expected, in the most commonly adopted order,[5] are $g_{9/2}$, $i_{11/2}$, $j_{15/2}$, $d_{5/2}$, $s_{1/2}$, $g_{7/2}$, and $d_{3/2}$. One immediately notes that the number of strongly excited levels observed (seven) is just the number of single-particle levels expected, so that there is just one nuclear level for each single-particle level.

[5] S. G. Nilsson, Kgl. Danske Videnskab. Selskab, Mat.-fys. Medd. **29**, No. 16 (1955).

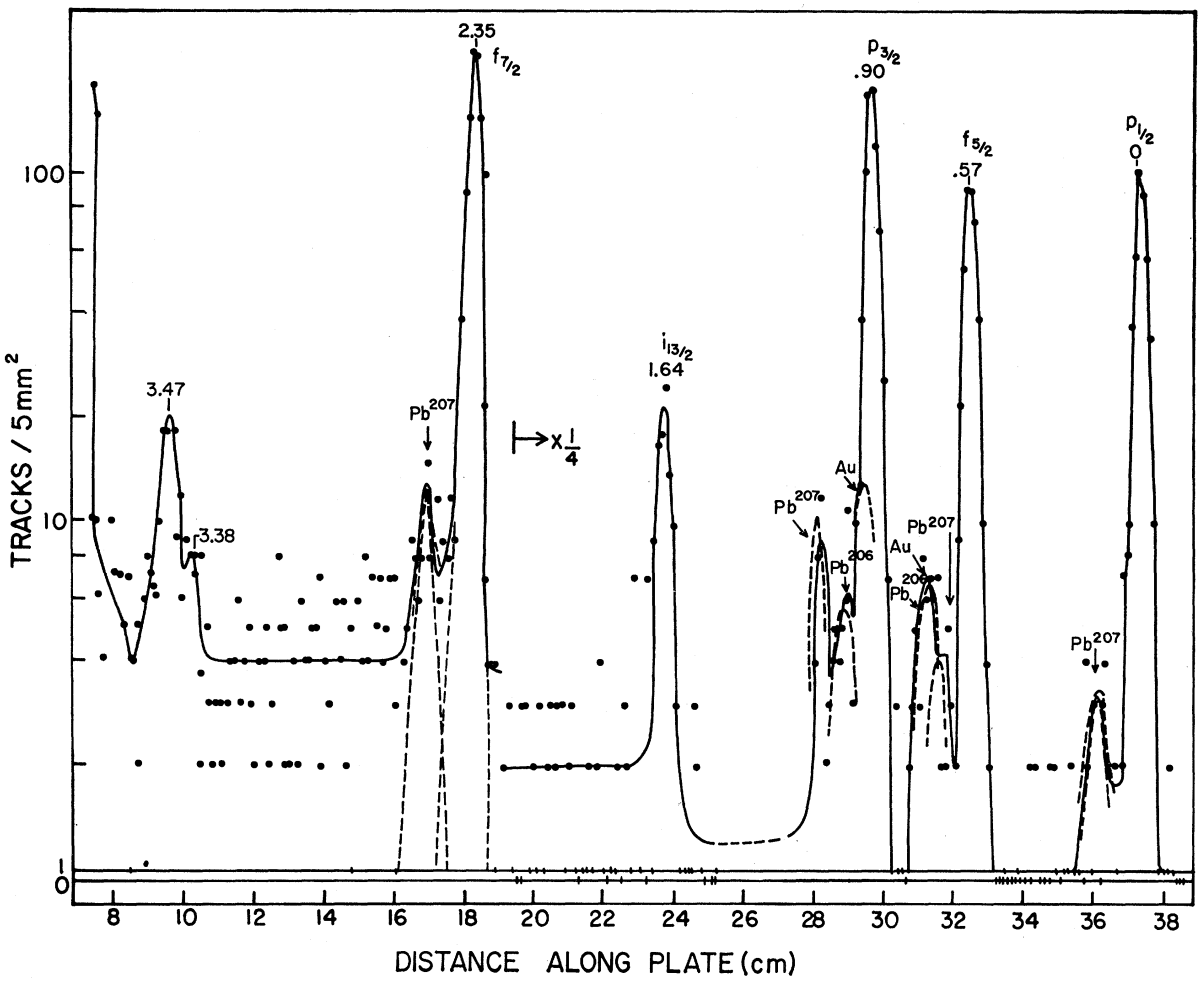

FIG. 2. Triton energy spectrum in $Pb^{208}(d,t)Pb^{207}$ at 90°. The well-known single-particle levels in Pb^{207} are labeled against the triton groups together with their excitation energies in MeV. The impurity lines due to Au backing, Pb^{207}, and Pb^{206} are also shown.

This is a very unique situation; ordinarily one might expect states based on a coupling of excited states of Pb^{208} with the single neutrons to give levels which mix with the simple single-particle levels so that both are excited in (d,p) reactions. However all of the states of Pb^{208} up to about 4-MeV excitation have negative parity, so that when they couple with the $g_{9/2}$ or $i_{11/2}$ particles, they can only form negative-parity states, which can mix only with the $j_{15/2}$. The lowest level of this type is at ~2.6-MeV excitation which is too far from where the $j_{15/2}$ will be shown to be (1.41 MeV) to get appreciable mixing. (From giant resonance theory[6] one expects mixing over ~0.5 MeV at this excitation energy.[4]) In addition, one might expect positive parity levels from a coupling of the 2.6-MeV 3^- state of Pb^{208} with the $j_{15/2}$ level; these might mix with the principal single-particle states. However, these states would be at ~4.0-MeV excitation, and the minimum spin would be 9/2 so that it could mix only with the $g_{9/2}$ state, 4 MeV away. The lowest positive-parity state that can mix with the levels near the top of the shell (e.g., the $g_{7/2}$) are expected from a coupling of the 3.2-MeV, 5^- state of Pb^{208} with the $j_{15/2}$, which would be at an excitation of 4.6 MeV, or 2.1 MeV above the highest single-particle level. Since giant resonance theory[6] gives a mixing only over ~1.2 MeV at this excitation energy,[4] it is not surprising that there is only one nuclear level observed in Fig. 1 for each single-particle state.

The problem thus reduces to determining which of the observed levels corresponds to which of the single-particle levels. Two techniques are used in this identification, angular distributions and cross sections. We now discuss them in turn.

1. *Angular-Distribution Evidence*

Observed angular distributions for the various levels are shown in Fig. 3; this is reproduced from reference 1 except that the data for the 2.5-MeV level in that paper

[6] A. M. Lane, R. G. Thomas, and E. P. Wegner, Phys. Rev. **98**, 693 (1955).

were divided between the 2.47- and 2.52-MeV levels by determining the ratios between their intensities at several angles. The DWB calculated angular distributions are shown in Fig. 4. In comparing Figs. 3 and 4 and recognizing that no $l=1$ or 3 states are expected, one can immediately identify the 2.03-MeV level as $s_{1/2}$, and the 1.56-MeV level as a d state, almost certainly $d_{5/2}$ as it is the lowest energy d state. These assignments from angular distributions have been made previously by Miller, Wegner, and Hall.[7] The $d_{3/2}$ state should be comparable in cross section with the $d_{5/2}$, and the $g_{7/2}$ state should be comparable in cross section with the ground state which is known to be $g_{9/2}$ so that between the 2.47- and 2.52-MeV states one must be $d_{3/2}$ and the other $g_{7/2}$. The choice between the two alternatives is clear in comparing Figs. 3 and 4. The small-angle behavior of the two angular distributions is quite different, and completely consistent with assigning the 2.52-MeV state as $d_{3/2}$ and the 2.47-MeV state as $g_{7/2}$. Even the difference between the experimental and theoretical curves are in the direction expected from the discrepancy in Q values.

The DWB calculations were based on parameters derived from elastic scattering measurements; no attempt was made to adjust these to fit the present data, so that the detailed agreement between observed and calculated cross sections is far from perfect. In order to compare cross sections, it was therefore decided to compare only the average cross sections in the region between 45° and 90°. Since this region is the predominant contributor to the total cross section and the calculated angular distributions at back angles are rather

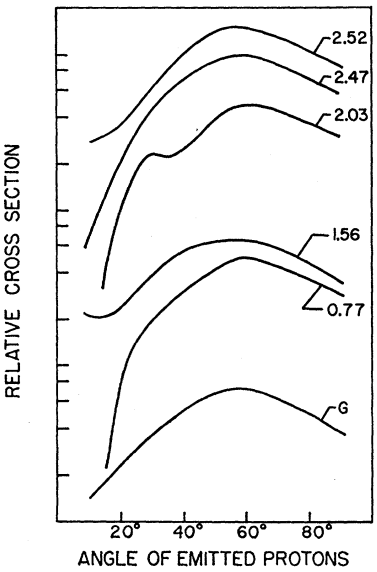

FIG. 3. Observed angular distributions of the various proton groups from $Pb^{208}(d,p)Pb^{209}$. Numbers attached to curves are excitation energies in MeV.

[7] D. W. Miller, H. E. Wegner, and W. S. Hall, Phys. Rev. **125**, 2054 (1962).

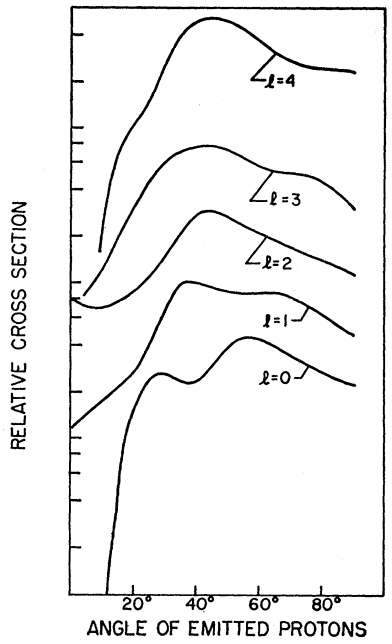

FIG. 4. Theoretical angular distributions of the protons for different orbital angular momenta l of the captured neutron in $Pb^{208}(d,p)Pb^{209}$, calculated by DWB approximation.

similar, the total cross section from the DWB calculations were used.

Since DWB calculations are available only for $Q=0,2,4$ MeV, and $l=0,1,2,3,4$, extrapolations are needed. Plots of σ_T vs Q for a given l give straight lines on a semilog plot in the range studied, so these lines were used for extrapolations. There should be little error in this process, as the largest extrapolation is 0.9 MeV.

The extrapolation to larger l is more difficult, and this is necessary to decide which of the remaining two observed levels, 0.77 MeV and 1.41 MeV, is $i_{11/2}$ and which is $j_{15/2}$. The extrapolation procedure is shown in Fig. 5. The average cross section for these levels is used to determine a point (black dot) at their average Q value (0.5 MeV) and their average l value (6.5). Calculations of σ_T for $l=0$–4 are then extrapolated to include this point. While this procedure is quite crude, its results are needed below in only the crudest way.

The comparison between observed and calculated cross sections is shown in Table I. Since ratios of cross sections are most accurately determined experimentally and most meaningful theoretically (in the present stage of the calculations), all cross sections are given as the ratio to the 1.56-MeV level.

Among the more strongly excited levels, the agreement between experiment and theory is very good. The assignment of 1.56 MeV as $d_{5/2}$ rather than $d_{3/2}$ is ascertained, and the choice between the $d_{3/2}$ and $g_{7/2}$, decided on above from angular distributions, is very strongly corroborated. For the $i_{11/2}$ and $j_{15/2}$ states one cannot expect such good agreement because of the crude

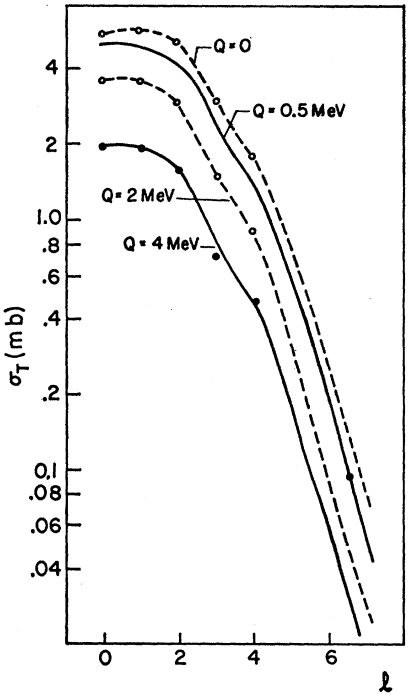

FIG. 5. Extrapolation of dependence of total (d,p) cross sections on l. Points from $l=0$ to 4 are from DWB calculations; point at $l=6.5$ is average of cross sections for two levels known to be either $l=6$ or $l=7$. See discussion in text.

extrapolation used for the calculated cross sections. However, if one must only choose between the two possible assignments, the results shown in Table I, where calculations based on both assumptions are given, strongly indicate that the 0.77-MeV state is $i_{11/2}$ and the 1.41-MeV state is $j_{15/2}$.

Thus, the level scheme for Pb^{209} is as shown in Fig. 6. The 2.15-MeV state is excited very weakly here (about 30 times less than the 2.03-MeV state), but it is the principal state[8] populated in the beta decay of Tl^{209}. It is known to be $1/2^-$ or $3/2^-$ since it decays by an $E1$ transition to the $s_{1/2}$ state; it is very probably $1/2^-$ because if it were $3/2^-$, it would almost surely have a strong branching to the $5/2^+$ state. Thus, we have here a peculiar situation where Tl^{209} decays by a first-forbidden transition when an allowed, non-l-forbidden transition is available with higher energy. The log ft for the transition to the 2.03-MeV state is larger than 6.4, which is probably the highest known for an allowed, non-l-forbidden transition. The reason, of course, is that the two states have different principal quantum numbers n; the transition to the 2.03-MeV state is, therefore, "n forbidden."

Since the gamma transition between the 2.03- and 1.56-MeV states is pure $E2$, its lifetime should be 2×10^{-9} sec and should therefore be observable by delayed coincidence following the 120-keV transition in the decay of Tl^{209}. It would be interesting to see whether a transition between two pure single-particle states goes at about the "single particle" transition rate.

TABLE I. Cross sections (averaged over 45–90°) for exciting various levels of Pb^{209} by $Pb^{208}(d,p)$ reactions.

Excitation energy (MeV)	Q (MeV)	Assumed state	$\bar{\sigma}/\bar{\sigma}(1.56)$ Exp.	Theor.
0	1.6	$g_{9/2}$	0.35	0.32
0.77	0.8	$i_{11/2}$	0.052	0.058
1.41	0.2	$j_{15/2}$	0.042	0.036
1.56	0	$d_{5/2}$	std.	1.00
2.03	−0.4	$s_{1/2}$	0.49	0.42
2.47	−0.9	$g_{7/2}$	0.59	0.58
2.52	−0.9	$d_{3/2}$	0.88	0.87
0.77	0.8	$j_{15/2}$	0.052	0.085
1.41	0.2	$i_{11/2}$	0.042	0.023

[8] *Nuclear Data Sheets*, National Academy of Sciences National Research Council (U. S. Government Printing Office, Washington, D. C., 1960).

B. Single-Particle States in Pb^{207}, Pb^{208}, and Bi^{210}

1. $Pb^{206}(d,p)Pb^{207}$ Reactions

The levels of Pb^{207} excited in the $Pb^{206}(d,p)$ reaction are listed in Table II; their positions and the cross sections for their excitation are shown in Fig. 7 where a similar plot for the $Pb^{208}(d,p)$ reaction is included for comparison. One immediately notes a strong similarity between the spectra obtained in these two cases, and this can be used to identify the strongest peaks as a coupling of the ground state of Pb^{206} with the various single-particle states in the $N=126$–184 shell (cf Table I). In addition, many weakly excited states are observed. This is to be expected, since there should be several states from the coupling of each state of Pb^{206} with each of the single-particle states, and some of these would have the same spin and parity as the principal

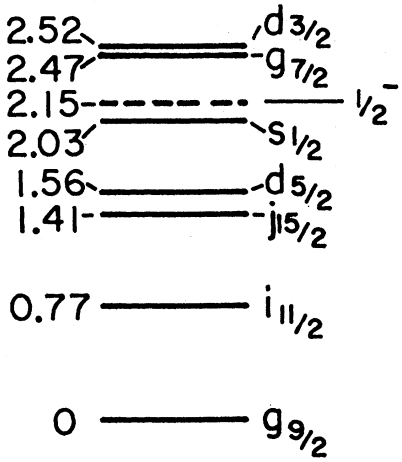

FIG. 6. Single-particle levels in Pb^{209} observed in $Pb^{208}(d,p)$. The dashed line corresponds to the weakly excited state known from the beta decay of Tl^{209}.

TABLE II. Energy levels in Pb^{207} (above 2.7 MeV) excited by $Pb^{206}(d,p)$ reactions. Relative yields are at 60°.

Excitation energy (MeV)	Relative yield	S.P. state	Excitation energy (MeV)	Relative yield	S.P. state
2.74	68	$g_{9/2}$	4.69	16	
3.47	8		4.74	16	
3.62	34	$i_{11/2}$	4.94	18	
3.70	7		5.03	23	
3.81	10		5.08	23	
4.02	8		5.13	57	$g_{7/2}$
4.10	13		5.18	154	$d_{3/2}$
4.29	30	$j_{15/2}$	5.26	24	
4.36	164	$d_{5/2}$	5.29	26	
4.43	16		5.36	14	
4.51	22		5.44	15	
4.60	160	$s_{1/2}$	5.52	18	

single-particle states and would therefore mix with them. For example, the 2^+ first-excited state of Pb^{206} (0.80 MeV) should couple with the $g_{9/2}$ single-particle state to give $5/2^+$, $7/2^+$, $9/2^+$, $11/2^+$, $13/2^+$ levels about 0.8 MeV above the principal $g_{9/2}$ state. One would therefore expect a strong mixing between the $11/2^+$ state of this group and the $i_{11/2}$ single-particle state, so that both of these states would share the $i_{11/2}$ single-particle strength. Since the level density of Pb^{206} is

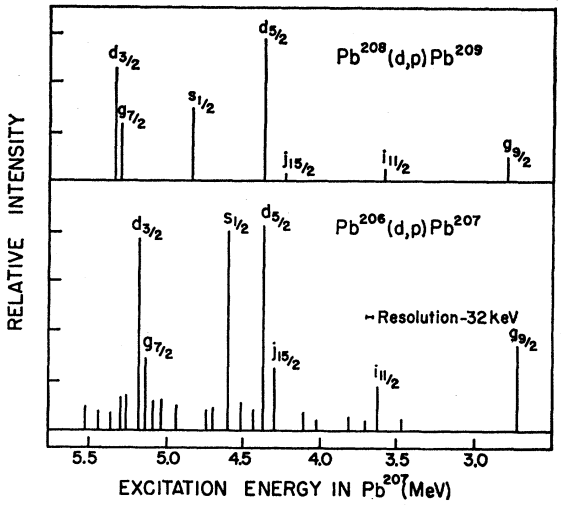

FIG. 7. The low-energy part of the proton spectra from $Pb^{206}(d,p)Pb^{207}$ at 60°. For comparison the $Pb^{208}(d,p)$ spectrum is also included for the same angle, which is plotted in the same Q-value scale. The probable single-particle states in Pb^{207} for $N>126$ shells are also indicated.

rather large,[9] one expects a great many weakly excited levels, in accordance with observation.

It is interesting to attempt to explain the shifts in

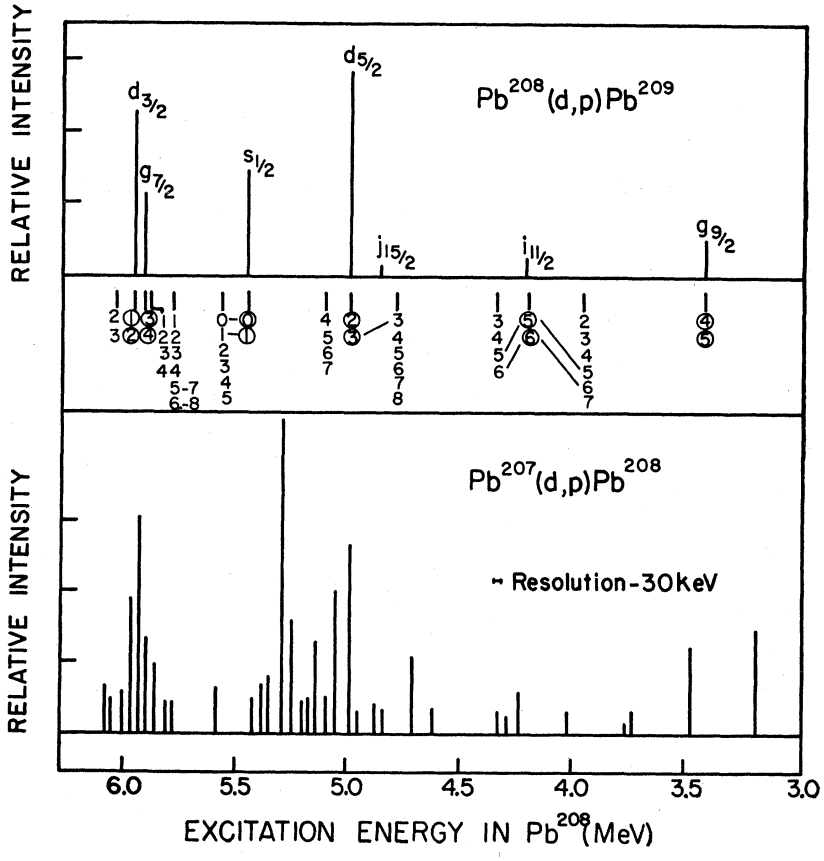

FIG. 8. (Bottom) The low-energy part of the proton spectra from $Pb^{207}(d,p)Pb^{208}$ at 60°. (Middle) The possible unperturbed negative-parity states according to the shell model, which are expected to be excited in (d,p) reactions. The numbers listed below each level are the spin values. The encircled spin states are from a $(p_{1/2}^{-1}j)$ admixture. States connected by lines are expected to mix with them. (Top) The single-particle states in Pb^{209} excited in $Pb^{208}(d,p)$ reactions at 60°, plotted in the same Q-value scale.

[9] W. W. True and K. W. Ford, Phys. Rev. **109**, 1675 (1958).

TABLE III. Energy levels of Pb^{208} (above 3 MeV) excited by $Pb^{207}(d,p)$ reactions. Relative yields are at 60°.

Excitation energy (MeV)	Relative yield	Excitation energy (MeV)	Relative yield
3.19	29	5.16	10
3.47	24	5.20	9
3.73	6	5.24	32
3.76	2	5.28	88
4.01	5	5.34	16
4.22	12	5.37	14
4.28	5	5.41	10
4.32	6	5.58	13
4.61	7	5.77	9
4.70	21	5.80	9
4.83	6	5.85	19
4.86	8	5.89	27
4.94	7	5.93	61
4.98	53	5.96	38
5.03	40	6.00	12
5.08	10	6.05	10
5.12	26	6.07	14

the $s_{1/2}$, $d_{3/2}$, and $g_{7/2}$ states in Pb^{207} relative to those states in Pb^{209}. The simplest calculation is to take into account the coupling with a collective core oscillation. If one uses the parameters of True and Ford,[9] an energy shift of 0.18 MeV is found for the $s_{1/2}$ state. This is in very satisfactory agreement with the observed shift of about 0.20 MeV. It should also be noted that this coupling with the core oscillation predicts energy shifts in the $g_{7/2}$ and $d_{3/2}$ states, but not in the other single-particle states, all in accordance with observation.

2. $Pb^{207}(d,p)Pb^{208}$ *Reactions*

The levels of Pb^{208} excited in the $Pb^{207}(d,p)$ reaction are listed in Table III, and Fig. 8 shows a comparison between the results of this reaction and $Pb^{208}(d,p)$. If we ignore mixing, each level of angular momentum j in the latter reaction should correspond to two levels in the former with spins $(j+1/2)$ and $(j-1/2)$, since the ground state of Pb^{207} is a very pure $(p_{1/2})^{-1}$. These states, with the exception of those arising from $j_{15/2}$, are shown encircled in the center part of Fig. 8. The two lowest lying Pb^{208} states shown are thus the $(g_{9/2}p_{1/2}^{-1})$ coupling to 5^- and 4^-; according to usual coupling rules,[10] the former should lie lower. These states are also excited in the beta decay of Tl^{208}, and from the decay scheme studies they have been determined to be 5^- and 4^- in the order expected. To understand the higher excited states, one must take into account levels formed from couplings of the various hole states of Pb^{207} with the various particle states j. The unperturbed positions of the negative-parity states of this type are shown in the center part of Fig. 8 with the various spins that can be formed from the coupling. When these states lie close in energy to encircled states, one can expect mixing so that the $(p_{1/2}^{-1}j)$ shell-model state will be distributed among them and they will all be excited in (d,p) reactions. For example, the 5^- and 6^- states formed from $(p_{1/2}^{-1}i_{11/2})$ would mix with states of these spins and parity from $(f_{5/2}^{-1}g_{9/2})$ and $(p_{3/2}^{-1}g_{9/2})$ as shown by the lines in Fig. 8. We thus expect to excite a total of six states in this energy region, five of which are observed including one known to be 5^- from the decay scheme of Tl^{208}. It is curious, however, that a state at 3.96 MeV[8] identified as 6^- from the decay scheme of Tl^{208} is not observed.

Note added in proof.—Detailed shell-model calculations by Pinkston and True (private communication) have shown that this level has very little $(p_{1/2}^{-1}j)$ in its configuration. This explains why it is not excited here.

The predictions of this very simplified model are not so successful with the more highly excited states. It predicts very little mixing for the $d_{5/2}$ state, whereas the observed mixing seems to be relatively strong in that several states in its energy region are about equally excited. On the other hand, our model predicts that the $s_{1/2}$ state should be mixed among at least four states, but one state is observed to be very strongly excited. In the $d_{3/2}$–$g_{7/2}$ energy region, one expects and finds very extensive mixing (14 states predicted, 9 observed).

The $j_{15/2}$ state has not been considered here as it leads to positive-parity states in this region and the total excitation of these states would be quite small. However, some of the observed states shown in Fig. 8 must be due to excitation of this state. The $(p_{1/2}^{-1}j_{15/2})$ coupling leads to 7^+ and 8^+ states; in this energy region, states of these spins and parity would also arise from $(i_{13/2}^{-1}g_{9/2})$, so that there should be mixing and four states should be observed.

In general, it is clear that the number of observed

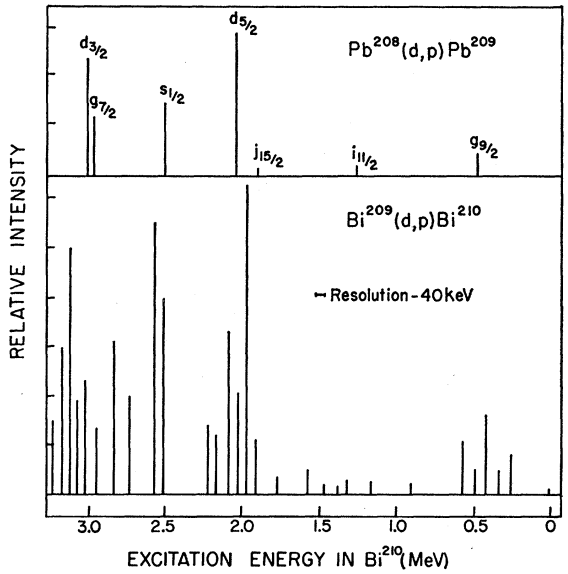

FIG. 9. The proton spectrum in $Bi^{209}(d,p)Bi^{210}$ at 60°. For comparison the $Pb^{208}(d,p)$ spectrum is also plotted in the same energy scale for the same angle.

[10] D. Kurath, in *Nuclear Spectroscopy* (Academic Press Inc., New York, 1960).

states is somewhat fewer than the number predicted. This is undoubtedly due to lack of resolution in the experiment; the resolution obtained here is about 30 keV.

3. $Bi^{209}(d,p)Bi^{210}$ Reactions

The energy levels of Bi^{210} excited in the $Bi^{209}(d,p)$ reaction are shown and compared with the levels from $Pb^{208}(d,p)$ in Fig. 9; they are also listed in Table IV where they are compared with the recent MIT work.[11] Since the ground state of Bi^{209} is $h_{9/2}$, one expects the $g_{9/2}$, $i_{11/2}$, and $j_{15/2}$ single-particle states to have 10 components each before considering mixing. Above about 0.9 MeV, one expects nearly an equal number of additional levels from mixing with states in which the proton is excited to the $f_{7/2}$ level. For the $(g_{9/2}h_{9/2})$ group, all 10 states appear in the MIT work[11] although only seven are resolved in this work. However only a small fraction of the states expected from $(h_{9/2}i_{11/2})$ and $(h_{9/2}j_{15/2})$ are observed even though the resolution does not appear to be the limiting factor. The level groups from $(h_{9/2}d_{5/2})$, $(h_{9/2}s_{1/2})$, and the $(h_{9/2}g_{7/2})$-$(h_{9/2}d_{3/2})$ pair all seem to be well separated from one another, although the number of components in each group is somewhat less than expected when mixing is considered.

C. Single-Particle States in the $N>184$ Shell

In the spectrum from $Pb^{208}(d,p)Pb^{209}$, there is an energy gap of 1.45 MeV between the $d_{3/2}$ single-particle state and the next strongly excited level. This presumably is the gap between the $N=126$–184 shell and the $N>184$ shell, so that the 3.97-MeV state marks the beginning of the $N>184$ shell. The levels observed in it and their relative excitation cross sections are listed in Table V. Unfortunately, one expects (and finds) strong mixing in this region with levels arising from excitation of neutrons from the $82<N\leqslant 126$ shell to the $126<N\leqslant 184$ shell, and from excitation of protons from the $50<Z\leqslant 82$ to the $82<Z\leqslant 126$ shell. The spectrum is therefore very complicated and very little can be learned from it at present.

TABLE IV. Energy levels of Bi^{210} excited by $Bi^{209}(d,p)$ reactions. Relative yields are at 60°.

Energy (this work) (MeV)	Energy (reference 11) (MeV)	Relative yield	Energy (this work) (MeV)	Energy (reference 11) (MeV)	Relative yield
0	0	4	1.976	1.969	252
				1.977	
...	0.051	...	2.024	2.024	83
0.270	0.270	35	2.088	2.071	133
				2.099	
0.340	0.321	21	2.170	2.169	49
	0.347				
0.426	0.434	66	2.227	2.229	57
0.488	0.502	22	2.518	2.514	160
0.570	0.547	43	2.576	2.569	222
	0.588			2.601	
0.902	0.915	10	2.737	2.723	79
				2.751	
1.166	...	12			
1.317	...	12	2.833	2.828	125
1.371	1.374	8	...	2.909	...
1.462	1.461	8	2.945	2.955	54
...	1.514	...	3.020	3.001	92
				3.026	
1.566	1.576	21			
1.760	...	15	3.078	3.058	77
				3.091	
1.912	1.914	45			
			3.127	3.127	200
			3.173	3.172	120
			3.238	3.233	60

TABLE V. Energy levels of Pb^{209} (above 3-MeV excitation energy) excited by $Pb^{208}(d,p)$ reactions. (The relative yield for 2.03-MeV $s_{1/2}$ state is 306 at the same angle.)

Excitation energy (MeV)	Relative yield at 60°
3.97	26
4.10	38
4.28	23
4.44	27
4.66	9
4.73	16

D. Ground-State Configuration of Pb^{206}

The $Pb^{206}(d,p)$ reaction leading to the single-hole states of Pb^{207} may be used to determine the ground-state configuration of Pb^{206}. This is especially interesting since there are shell-model and pairing theory calculations of this configuration available for comparison.

The Pb^{206} ground-state wave function may be written

$$\psi_{206}=a(p_{1/2})^{-2}+b(f_{5/2})^{-2}+d(p_{3/2})^{-2}+e(i_{13/2})^{-2}+f(f_{7/2})^{-2}.$$

Two methods for determining the coefficients in this expression from (d,p) reactions are used in reference 1; both of them may be improved by use of the DWB calculations. One method depends on the comparison between cross sections for the ground-state transitions in $Pb^{206}(d,p)$ and $Pb^{207}(d,p)$ reactions; this should be

$$\sigma(206)/\sigma(207)=2.55a^2,$$

where the deviation of 2.55 from 2.00 is determined by the Q-value dependence of the (d,p) cross section for $l=1$. In reference 1, a rather crude method for determining this Q-value dependence was used, and the coefficient was 2.43. The DWB calculations should give a fairly reliable representation of the Q-value dependence, and it was from them that the 2.55 was obtained. The experimental cross-section ratio, given in reference 1, is 1.44; this corresponds to $a^2=0.56$.

The second method depends on the comparison of cross sections for $Pb^{206}(d,p)$ leading to the various single-hole states of Pb^{207}. If the l dependence and Q-value dependence of the (d,p) cross section are known, the ratios of these cross sections gives the ratio $a^2:b^2:d^2:e^2:f^2$. The normalization condition then determines these coefficients absolutely. In reference 1, the

[11] J. R. Erskine, Massachusetts Institute of Technology, Laboratory of Nuclear Science, Progress Report, May 1, 1961 (unpublished), p. 116.

TABLE VI. Coefficients in ground-state wave function of Pb^{206}.

Coeff.	State	From data at 30°	45°	60°	75°	90°	av	Adj. av	Shell-model calculations True and Ford[a]	Kearsley[b]	Guman *et al.*[c]
a^2	$p_{1/2}$	0.51	0.47	0.57	0.44	0.45	0.49	0.54	0.73	0.70	0.74
b^2	$f_{5/2}$	0.17	0.21	0.20	0.26	0.27	0.23	0.20	0.13	0.11	0.14
d^2	$p_{3/2}$	0.12	0.10	0.12	0.13	0.14	0.12	0.12	0.13	0.14	0.11
e^2	$i_{13/2}$	0.19	0.19	0.09	···	0.11	0.14	0.12	0.009	0.02	0.002
f^2	$f_{7/2}$	···	0.03	0.02	0.05	0.03	0.033	0.03	···	0.02	0.005

[a] See reference 9.
[b] See reference 12.
[c] See reference 13. In this case the configuration is different, since coupling with one and two phonons are considered. We have used $\Sigma_{j_2JR}[C^0(j_1j_2J,NR)]^2$ as the total strength for exciting the j_1 state.

methods of estimating the l dependence and Q dependence were quite crude; the calculations were therefore repeated using the DWB results. Since no DWB results were available for the $i_{13/2}$ state, an extrapolation similar to that in Fig. 5 was used. The shape of the angular distribution also had to be estimated by extrapolation, so that the values of e^2 are somewhat more questionable than for the other coefficients.

An independent set of parameters was determined at each of the following angles: 30, 45, 60, 75, and 90°. The results are shown in Table VI. The variation of these results with angle is not too large, and is easily explained by the fact that the DWB does not give a good fit to the angular distributions as discussed above. The next column of Table VI gives the average value of the coefficients over the angles where measurements were made.

The value of a^2 comes out as 0.49 which is somewhat lower than the determination of a^2 (0.56, 0.54) by the other two methods described in this paper [one just above, the other from $Pb^{207}(d,t)$ discussed below] although the discrepancy is not unduly large considering the crudity of the technique used to obtain Table VI. Taking account of the other determinations, we estimate a weighted average value of $a^2=0.54$. This change must be compensated by reducing the other coefficients; however, the coefficient d^2 for the $p_{3/2}$ state should be rather better determined in Table VI than the others since its angular distribution is similar to that of the ground state. Therefore, this coefficient was not adjusted, and all others were adjusted in the same ratio to compensate the increase in a^2. The resulting coefficients are given in the "adjusted average" column of Table VI. These may then be compared with the shell-model calculations of True and Ford,[9] of Kearsley[12] and of Guman *et al.*[13] shown in the following three columns.

The discrepancy between the experimental and theoretical wave functions of the ground state of Pb^{206} is considerably larger than expected. The direction of the discrepancy suggests that the strength of the short-range residual interaction should be increased to get more mixing. This would destroy the very good agreement between theory and experiment on the level structure of Pb^{206}, but this could perhaps be restored by taking into account the effect of short-range hard-core repulsion in the residual interaction.[14]

From the standpoint of pairing theory,[15] the coefficients found in Table VI are related to U_j^2, the complement of the occupation number, by a factor of $(j+1/2)$. Thus, the results of Table VI correspond to $U_{1/2}^2=0.54$, $U_{5/2}^2=0.066$, $U_{3/2}^2=0.060$, $U_{13/2}^2=0.019$, and $U_{j/2}^2=0.0075$. If one takes the observed levels of Pb^{207} as the unperturbed single-particle energies, these results are roughly reproduced with $\Delta=0.40$. This corresponds to $G=0.132$, or $27/A$, which is not out of line with expectations.

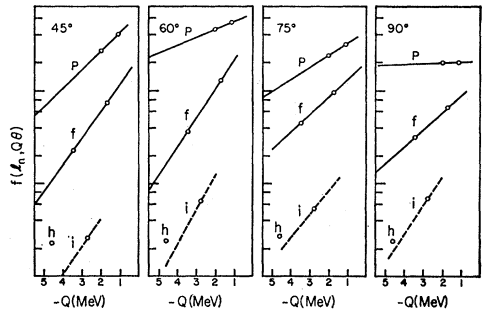

FIG. 10. Plots of $f(l_n,Q,\theta)$ vs Q for different states excited in $Pb^{208}(d,t)Pb^{207}$ at various angles of observation. The circle marked with "h" is the 3.47-MeV level.

RESULTS AND DISCUSSIONS: (d,t) REACTIONS

The differential cross section for a (d,t) reaction may be expressed as[1]

$$d\sigma/d\omega=f(l_n,Q,\theta)Sc^2, \quad (1)$$

where S is the coefficient of fractional parentage (c.f.p.) between the final state and the initial state plus a neutron hole, c is the overlap integral between the initial state minus the neutron and the final state, and the term $f(l_n,Q,\theta)$ is a generalization of the Butler stripping term which arises from the mechanism of the pickup process. It is a function of the orbital angular momen-

[12] J. Kearsley, Nuclear Phys. **4**, 157 (1957).
[13] V. N. Guman, Y. I. Kharitonov, L. A. Sliv, and G. A. Sogomonova, Nuclear Phys. **28**, 177 (1961).
[14] L. Silverberg, Arkiv Fysik **20**, 355 (1961).
[15] L. S. Kisslinger and R. A. Sorenson, Kgl. Danske Videnskab. Selskab, Mat.-fys. Medd. **32**, No. 9 (1960).

tum of the picked-out neutron l_n, the scattering angle θ, and the energy released in the reaction Q. It also depends on the nuclear radius R_0, but for the analysis of Pb isotopes we have assumed R_0 as a fixed quantity.

A. Single-Hole States in the $82<N\leqslant 126$ Shell from $Pb^{208}(d,t)Pb^{207}$

The $Pb^{208}(d,t)$ reaction should excite only the single-hole states in Pb^{207}; from the shell model one expects the $p_{1/2}$, $f_{5/2}$, $p_{3/2}$, $i_{13/2}$, $f_{7/2}$, and $h_{9/2}$ states in this region. All of these states are well known from decay scheme work[8] except the $h_{9/2}$; in this section we therefore discuss the identification of this missing level.

It is clear from the outset that the $h_{9/2}$ level cannot lie below 2.4-MeV excitation or else it would be excited in the beta decay of Bi^{207}. It therefore was expedient to look at higher excitation energies. A preliminary search with the $Pb^{208}(d,t)$ reaction revealed a triton group at an excitation energy of 3.47 MeV. We now cite the evidence that this level is indeed the $h_{9/2}$ single-hole level.

The expected cross section for exciting the $h_{9/2}$ hole level may easily be estimated. For all single-hole levels, $S=c=1$ in Eq. (1) so that a cross section measurement gives a direct determination of $f(l_n,Q,\theta)$. By determining $f(l_n,Q,\theta)$ for the various known hole levels, a systematics for this function can be set up as was done in reference 1. This is shown for four angles in Fig. 10. From this systematics, the cross section for the $h_{9/2}$ state can be estimated as a function of the Q value. The cross section for the observed 3.47-MeV state is shown in the figure; it clearly is of about the correct size.

The next question to settle was whether there are any other triton groups of sufficient intensity to be the $h_{9/2}$ hole state. The region of excitation above 3.6 MeV could not be investigated with photographic plate detection as this technique does not easily distinguish between particles, and in that energy region there are deuterons (from elastic and inelastic deuteron scattering) with the same magnetic rigidity. The spectrograph was therefore converted to a spectrometer using a CsI scintillation crystal as detector. This easily discriminates between deuterons and tritons of the same magnetic rigidity on the basis of pulse height—the deuterons have 1.5 times higher energy and therefore produce pulses 1.5 times larger. The triton spectrum from a natural Pb target was then studied over a large energy range by changing the field of the spectrometer magnet in small steps.

The pulse-height range of tritons was checked at frequent intervals by measuring the spectrum from a Be target which produces a continuous distribution of tritons.

The results of this measurement are shown in Fig. 11. There is clearly no other triton group as large as 10% of the 3.47-MeV group up to at least an excitation of 5.5 MeV, whereas from Fig. 10, one would expect the $h_{9/2}$ hole state to be at least 1/4 as strongly excited as the 3.47-MeV state even if its excitation energy where as high as 5.5 MeV. Thus there is no other triton group up to 5.5-MeV excitation energy which could possibly be the $h_{9/2}$ hole state.

There is one other expected property of the $h_{9/2}$ hole state that can easily be checked—it should occur at the same energy and with about the same cross section in the (d,t) reactions in Pb^{206}, Pb^{207}, Pb^{208}, and Bi^{209}. This was investigated and verified. In addition this level appears regularly in energy and cross section in (p,d) reactions on all of these isotopes.[16]

In summary, the 3.47-MeV state has the cross section expected for the $h_{9/2}$ hole state, whereas no other triton group up to quite high excitation energy has nearly sufficient cross section; and an analog level occurs regularly in energy and cross section in all four isotopes in which it is expected. This is very convincing evidence that the 3.47-MeV level of Pb^{207} is indeed the $h_{9/2}$ hole state.

B. $Pb^{207}(d,t)Pb^{206}$

The spectrum of Pb^{206} is more difficult to understand theoretically. Since the ground state of Pb^{207} is $p_{1/2}^{-1}$, in the (d,t) process states like $(p_{1/2}p_{1/2})^{-1}$, $(p_{1/2}f_{5/2})^{-1}$, $(p_{1/2}p_{3/2})^{-1}$, etc., are excited in Pb^{206}. Table VII summarizes the energies of the levels of Pb^{206} observed in (d,t) reaction. In the second column some of these levels known[17] from the decay of Bi^{206} are listed. The theoretical level positions of True and Ford, and those of Guman and co-workers[13] are given in the next two columns for comparison. The fifth column lists the theoretical spins and parities for these levels. These

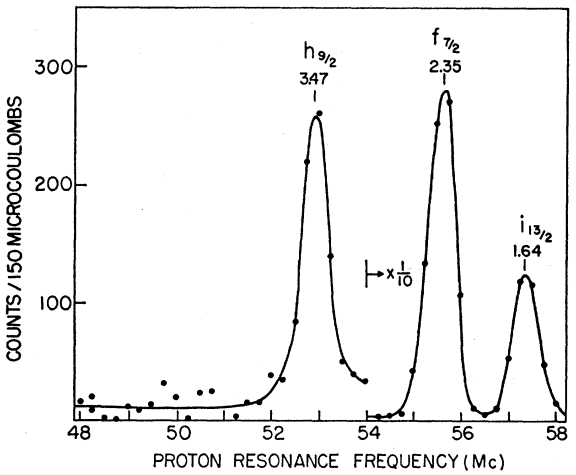

FIG. 11. The low-energy part of the triton spectra observed in $Pb(d,t)$ reactions at 90°, showing the presence of the $h_{9/2}$ neutron hole state in Pb^{207} together with the well-known $f_{7/2}$ and $i_{13/2}$ hole states.

[16] B. L. Cohen and S. W. Mosko, Phys. Rev. **106**, 995 (1957).
[17] D. E. Alburger and M. H. L. Pryce, Phys. Rev. **95**, 1482 (1954).

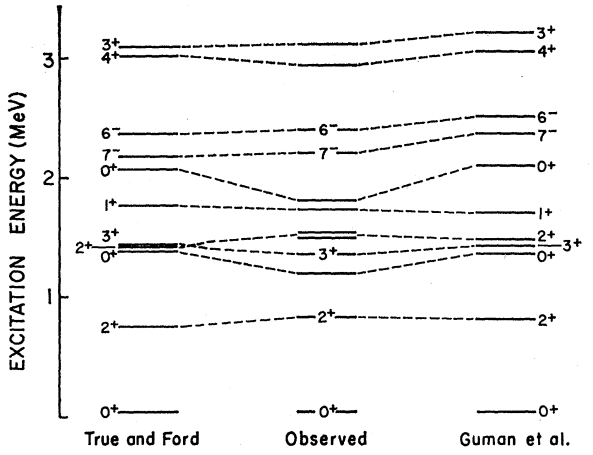

FIG. 12. Comparison of the energy levels of Pb^{206} observed in the $Pb^{207}(d,t)$ reactions with the theoretical level scheme of True and Ford, and of Guman *et al.* The latter are those states which have large $(p_{1/2}j)^{-1}$ admixtures.

theoretical levels are those which have a reasonably high $(p_{1/2}j)^{-1}$ admixture (last column), so that they are strongly excited in the (d,t) reaction. Figure 12 gives a comparison between the observed levels and the predicted scheme. The agreement is more or less satisfactory, but the 0^+ excited states are found to be more dispersed in the theoretical scheme.

In True and Ford's work, a singlet-even Gaussian interaction is assumed between the two neutron holes and harmonic oscillator wave functions are used to describe single-particle states. Moreover, they considered a weak coupling of the two neutrons with the one-phonon core excitation. In Guman's work[13] the residual interaction is also Gaussian, but the average single-particle potential is the more realistic Woods-Saxon potential with spin-orbit coupling. The parameters in this potential are determined from the fit with the single-particle spectra in Pb^{207}. They have taken an improved representation, with intermediate coupling of the two particles with the core. In True and Ford's calculation, the state of Pb^{206} is given by

$$|J\rangle=\sum_{j_1j_2} a_{j_1j_2}|j_1j_2J\rangle,$$

TABLE VII. Energy levels excited by (d,t) reaction in Pb^{207}.

Excitation energy (MeV) This work	Alburger[a]	True and Ford[b]	Guman[c]	Predicted[b] *I* II	True and Ford[b] configuration
0	0	0	0	0^+	$0.72p_{1/2}$
0.80	0.803	0.725	0.77	2^+	$0.56f_{5/2}+0.29p_{3/2}$
1.17		1.363	1.33	0^+	$0.17p_{1/2}$
1.34	1.341	1.404	1.39	3^+	$1.00f_{5/2}$
1.47		1.391	1.45	2^+	$0.37f_{5/2}+0.59p_{3/2}$
1.51					
1.71		1.745	1.71	1^+	$0.98p_{3/2}$
1.78		2.056	2.07	0^+	$0.09p_{1/2}$
2.19	2.200	2.166	2.33	7^-	$0.90i_{13/2}$
2.39	2.385	2.355	2.50	6^-	$0.97i_{13/2}$
2.93		3.010	3.02	4^+	$0.90f_{7/2}$
3.11		3.081	3.21	3^+	$1.00f_{7/2}$
4.07					

[a] See reference 17.
[b] See reference 9.
[c] See reference 13.

TABLE VIII. Cross section for various excitation in $Pb^{207}(d,t)$-Pb^{206} relative to that for $Pb^{208}(d,t)Pb^{207}$ ground state at respective angles.

Excitation energy (MeV)	90° meas.	90° calc.	75° meas.	75° calc.	60° meas.	60° calc.	45° meas.	45° calc.
0	0.30	0.38	0.30	0.40	0.32	0.43	0.33	0.53
0.80	0.38	0.71	0.39	0.68	0.41	0.65	0.33	0.52
1.17	0.25	0.09	0.18	0.09	0.16	0.09	0.14	0.05
1.34	0.29	0.57	0.37	0.45	0.41	0.39	0.21	0.24
1.47	0.75	0.83	0.73	0.82	0.67	0.81	0.62	0.45
1.51	0.37	···	0.54	···	0.35	···	0.15	···
1.71	0.51	0.68	0.57	0.60	0.57	0.68	0.49	0.34
1.78	0.07	0.04	0.13	0.04	0.06	0.04	0.08	0.03
2.19	0.10	0.09	0.10	0.06	0.06	0.04	0.02	0.01
2.39	0.10	0.09	0.07	0.06	0.06	0.04	0.02	0.01
2.93	0.22	0.30	0.19	0.22	0.16	0.16	0.10	0.07
3.11	0.19	0.25	0.09	0.17	0.13	0.13	0.10	0.06
4.07	0.02	···	0.02	···	<0.01	···	<0.01	···

whereas in the latter there are admixture of True and Ford states, given by

$$|I\rangle=\sum_{NRJ} a_{NRJ}(j_1j_2)|NR,(j_1j_2)J,I\rangle.$$

Since the number of phonons N is taken up to 2, the quantum number for angular momentum of core vibration R can be 0, 2, and 4. Thus, pure shell-model states $|j_1j_2J\rangle$ with $J=0$, 2, and 4 are mixed in this representation.

TABLE IX. Relative yields for $f_{5/2}$ and $p_{3/2}$ states in $Pb^{208}(d,t)$ and $Pb^{206}(d,t)$ reactions.

θ	$\sigma(f_{5/2})/\sigma(p_{3/2})$ $Pb^{208}(d,t)$	$\sigma(f_{5/2})/\sigma(p_{3/2})$ $Pb^{206}(d,t)$	$\sigma(p_{1/2})/\sigma(p_{3/2})$ $Pb^{206}(d,t)$	a^2
45°	0.43	0.66	0.23	0.72
75°	0.62	0.80	0.18	0.46
90°	0.51	0.76	0.25	0.52

Table VIII presents the differential cross sections for exciting various states of Pb^{206} relative to the ground-state transition in $Pb^{208}(d,t)Pb^{207}$. The theoretical cross sections are calculated from the paper of True and Ford[9] as described in reference 1, We may first note that the value of a^2, the fraction of the Pb^{206} ground-state wave function that is $(p_{1/2})^{-2}$, can be obtained as the ratio of observed to theoretical cross section for the ground-state excitation times the True-Ford value, $a_{TF}^2=0.73$. The observed to theoretical ratio averaged over angles is ~ 0.74, whence we find $a^2\simeq 0.54$. This is in good agreement with the results from the $Pb^{206}(d,p)$ reaction discussed above.

The results for most of the other levels in Table VIII are in reasonable agreement with theory. However, the predicted yield for the first 2^+ state is twice as large as compared to the actual value. In contrast to this, the 0^+ state at 1.17 MeV is found to be excited at a rate of 2.5 times the predicted rate. But the most disturbing observation is the location of a strongly excited level at 1.51 MeV. According to True and Ford[9] such a level cannot exist at this energy region and its origin is not very clear from the usual shell-model ideas.

TABLE X. Comparison of the energy levels of Pb^{205} excited in $Pb^{206}(d,t)$ reactions with the level scheme from Bi^{205} decay and shell-model prediction.

Excitation energy (MeV) This work	Herrlander[a]	Predicted energy True[b] (MeV)	Spin and parity Herrlander[a]	Single-particle state from (d,t) cross section	Relative yield in $Pb^{206}(d,t)$ at 75°
0	0	0	$5/2^-$	$f_{5/2}$	95
	0.0023	0.379	$1/2^-$	$p_{1/2}$	
0.26	0.2628	0.158	$3/2^-$	$p_{3/2}$	121
0.41	...	0.508 $(1/2^-)$	...		3
0.58	...	0.503 $(3/2^-)$	...		4
...	0.7033	0.746	$7/2^-$		...
...	0.7610	...	$(3/2^-)$		...
0.79	...	0.812 $(5/2^-)$	...		3
...	0.9876	0.938	$9/2^-$		...
1.00	1.0138	1.051	$13/2^+$	$i_{13/2}$	17
1.06	1.0437	1.043	$5/2^-$		3
...	1.4995	1.497 $(5/2^-)$	...		...
1.60	1.6146	1.706	$7/2^-$		7
1.76	1.7664	1.789	$7/2^-$	$f_{7/2}$	31
...	2.5665	2.557	$9/2^+$		...
...	2.6099	...	$9/2^+$		...
2.72	...	...	...	$h_{9/2}$	2

[a] See reference 19.
[b] See reference 18.

C. $Pb^{206}(d,t)Pb^{205}$

If we assume that the ground state of Pb^{206} is a pure $(p_{1/2})^{-2}$ configuration, then in the reaction $Pb^{206}(d,t)$, the $p_{1/2}^{-1}$ state would be obviously missing, and the spectra would look identical with $Pb^{208}(d,t)$ from $f_{5/2}$ onward. Actually this is evident from Fig. 13, which gives the observed spectra in $Pb^{206}(d,t)$, together with $Pb^{208}(d,t)$ spectra for comparison. The relative shifts of the single-particle states in the two cases could be qualitatively understood from the coupling of the neutron hole states with the 2^+ first phonon state in Pb^{206}. In a more quantitative way True[18] has extended the Pb^{206} calculation[9] to the three-neutron spectroscopy of Pb^{205}. Since the ground state of Pb^{206} contains appreciable admixtures of $(f_{5/2})^{-2}$, $(p_{3/2})^{-2}$, and $(i_{13/2})^{-2}$ (cf. Table VI), there should be a $p_{1/2}$ state strongly excited in $Pb^{206}(d,t)$ reaction. From Fig. 13 it is apparent that one of the two strongly excited low-lying states should contain this $p_{1/2}$ state. Our resolution (45 keV) indicates that it should be within 30 keV of either $f_{5/2}$ or $p_{3/2}$ state. From recent studies of Bi^{205} electron capture decay and Po^{209} α decay, Herrlander[19] has found a $1/2^-$ state at an energy of 2.3 keV above the ground state of Pb^{205}. This must be the $p_{1/2}$ state. Table IX presents the ratios of the yields of the $f_{5/2}$ and $p_{3/2}$ states excited in both $Pb^{208}(d,t)Pb^{207}$, and $Pb^{206}(d,t)Pb^{205}$ reactions. These should be approximately the same in both cases (assuming that the configuration mixing in Pb^{205} reduces the strengths of the $f_{5/2}$ and $p_{3/2}$ to the same extent and ignoring the small changes in the Q values). The third column of Table IX indicates that there is a definitely large admixture of the $p_{1/2}$ state in the observed ground-state excitation of Pb^{205}. The probable admixture (relative to the $p_{3/2}$ yield) is indicated in the next column. From this one can calculate the strength of the $(p_{1/2})^{-2}$ in Pb^{206} ground-state wave function (cf. Table VI), which is presented in the last column of Table IX. This is also an independent check that $a^2 \sim 0.54$ as found in the previous discussion. In Table X we have summarized our results and have compared them with the results of Herrlander[19] and the theoretical calculation of True.[18] It is a reassuring feature that our identifications of the single-particle states in Pb^{205} are in complete agreement with the energies, spins, and parities reported in Herrlander's works. But we do not understand why the 0.41-, 0.58-, and 0.79-MeV states are not observed in the decay of Bi^{205}. The general agreement with the theoretical calculations of True is very satisfactory, and it is very likely that the three

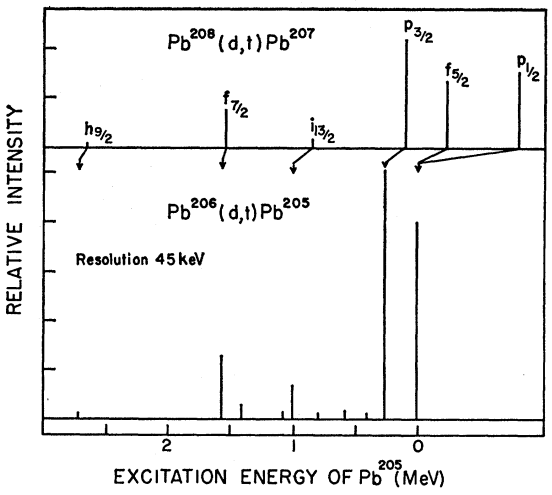

FIG. 13. The triton spectrum $Pb^{206}(d,t)Pb^{205}$ at 75°. For comparison the $Pb^{208}(d,t)Pb^{207}$ spectrum is also plotted in the same energy scale for the similar angle of observation. The arrows identify the single-particle states in Pb^{205}.

[18] W. W. True, Nuclear Phys. **25**, 155 (1961).
[19] C. J. Herrlander, Arkiv Fysik **20**, 71 (1961).

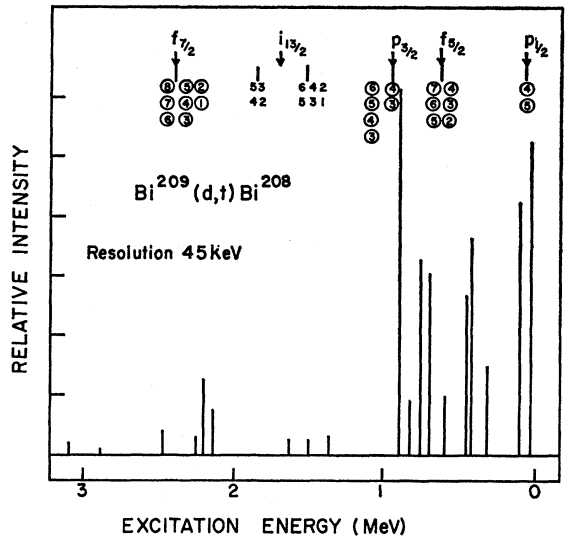

FIG. 14. The triton spectrum in $Bi^{209}(d,t)Bi^{208}$ at 45°. The possible unperturbed positive-parity states in Bi^{208} according to shell-model calculation are also listed together with their spin values. The encircled spin states are expected to be strongly excited in (d,t) reactions.

weak states mentioned above are the low-lying $1/2^-$, $3/2^-$, and $5/2^-$ states predicted by him (column 3 of Table X). These states should have a fairly large admixture of single-particle strengths and should be observed in (d,t) reactions. However, the predicted position of the $p_{1/2}$ state is far above the observed level. It will be interesting to see the effect of increasing the depth of the singlet even potential on this $1/2^-$ level. This will be consistent with our observation that there is more mixing in the ground state of Pb^{206}.

D. $Bi^{209}(d,t)Bi^{208}$

Shell-model calculations in Bi^{208} (and also in Bi^{210}) are more complicated since the two-particle interaction in this case is between a neutron and a proton. Thus the tensor force will play a prominent part in the spectroscopy of these nuclei. The positive parity levels in Bi^{208} will be given by the configuration mixing between the states $h_{9/2}p_{1/2}^{-1}$, $h_{9/2}f_{5/2}^{-1}$, $h_{9/2}p_{3/2}^{-1}$, $f_{7/2}p_{1/2}^{-1}$, $f_{7/2}f_{5/2}^{-1}$, $f_{7/2}p_{3/2}^{-1}$, and $h_{9/2}f_{7/2}^{-1}$. In the above the first term in each pair represents the proton state. The expected unperturbed positive-parity states resulting from this are shown in Fig. 14, which also includes the observed spectra in $Bi^{209}(d,t)$ for comparison. The states which are expected to be strongly excited are encircled. Thus the ground-state pair 4^+ and 5^+ are clearly resolved. Above this close doublet, and below 1 MeV, there should be 12 strongly excited states, but we observe only eight. This obviously indicates the necessity of a good energy resolution; in the present case the resolution is 45 keV. In the region between 1 to 2 MeV there is a broad continuum (whose height is approximately 2 in the scale of Fig. 14) above which the three levels are located. There is a possibility that we have missed many weaker levels in this region. Actually 10 negative-parity states (all of them weak) are expected in this region. The level spectrum above 2 MeV will be very complicated, but the four strongly excited states observed definitely corresponds to four of eight positive-parity states expected in this region. Table XI lists the excitation energies and the relative cross sections for the different states observed in $Bi^{209}(d,t)$ reactions.

TABLE XI. Energy levels excited in $Bi^{209}(d,t)Bi^{208}$.

Excitation energy (MeV)	Relative yield at 45°	Excitation energy (MeV)	Relative yield at 45°
0	104	1.35	6
0.07	84	1.49	5
0.29	29	1.62	5
0.40	72	2.14	15
0.43	53	2.20	25
0.58	19	2.25	6
0.68	60	2.47	8
0.75	65	2.89	2
0.82	18	3.10	4
0.88	122		

ACKNOWLEDGMENTS

The authors are greatly indebted to G. Fodor for preparing targets of the separated isotopes by evaporation, to R. H. Fulmer and A. L. McCarthy for help in exposing plates, and to G. R. Satchler and R. H. Bassel for providing the distorted-wave Born approximation calculations.